Science with the ASTRI Mini-Array: From Experiment to Open Observatory

Stefano Vercellone [†] [iD] on behalf of the ASTRI Project

INAF Osservatorio Astronomico di Brera, Via E. Bianchi 46, 23807 Merate, LC, Italy; stefano.vercellone@inaf.it;
Tel.: +39-02-72320-509

[†] http://www.astri.inaf.it/en/library/ (accessed on 21 January 2024).

Abstract: Although celestial sources emitting in the few tens of GeV up to a few TeV are being investigated by imaging atmospheric Čerenkov telescope arrays such as H.E.S.S., MAGIC, and VERITAS, at higher energies, up to PeV, more suitable instrumentation is required to detect ultra-high-energy photons, such as extensive air shower arrays, as HAWC, LHAASO, Tibet AS-γ. The Italian National Institute for Astrophysics has recently become the leader of an international project, the ASTRI Mini-Array, with the aim of installing and operating an array of nine dual-mirror Čerenkov telescopes at the Observatorio del Teide in Spain starting in 2025. The ASTRI Mini-Array is expected to span a wide range of energies (1–200 TeV), with a large field of view (about 10 degrees) and an angular and energy resolution of ∼3 arcmin and ∼10%, respectively. The first four years of operations will be dedicated to the exploitation of Core Science, with a small and selected number of pointings with the goal of addressing some of the fundamental questions on the origin of cosmic rays, cosmology, and fundamental physics, the time-domain astrophysics and non γ-ray studies (e.g., stellar intensity interferometry and direct measurements of cosmic rays). Subsequently, four more years will be dedicated to Observatory Science, open to the scientific community through the submission of observational proposals selected on a competitive basis. In this paper, I will review the Core Science topics and provide examples of possible Observatory Science cases, taking into account the synergies with current and upcoming observational facilities.

Keywords: ASTRI; imaging atmospheric Čerenkov arrays; very high-energy; γ-ray astrophysics; astro-particle

1. Introduction

About 300 celestial sources are currently known to emit in the $0.1 < E < 30$ TeV energy range (see the TeVCat Webpage[1] [1]) based on their detection by the major imaging atmospheric Čerenkov telescope arrays (IACTs), such as H.E.S.S. [2], MAGIC [3], and VERITAS [4], whose energy range extends up to a few tens of TeV. Alternatively, extended air shower arrays (EAS) such as HAWC [5], LHAASO [6] and Tibet AS-γ [7], adopt a different detection technique that allows us to investigate energies up to several hundreds of TeV, reaching the PeV limit. The sources detected by the current generation of EAS at energies $E > 100$ TeV, and up to a few PeVs are a factor of ten fewer.

The Čerenkov Telescope Array Observatory (CTAO [8]) will be the next large scale Čerenkov array and will cover an energy range from a few tens of GeV up to a few hundreds of TeV by means of telescopes of different sizes (see, e.g., [9]). It will be deployed in both hemispheres to observe the full sky. A few telescope prototypes were developed in recent years, among them the ASTRI-Horn dual-mirror, Schwarzschild–Couder (SC) telescope [10], currently operating on Mount Etna in Sicily (Italy), which obtained the first-light optical qualification by means of observation of Polaris, using a dedicated optical camera [11], and the first detection of very high-energy γ-ray emission from the Crab Nebula by a Čerenkov telescope in dual-mirror SC configuration [12].

In this review, I will first describe the ASTRI Mini-Array characteristics and performance in the context of currently available very high- and ultra-high energy (VHE and UHE, respectively) instrumentation (Section 2), then briefly highlight the ASTRI Mini-Array science topics that will be pursued during the first four years of operation (Section 3). In Section 4, I will describe in detail the subsequent four years of operation and the Open Observatory Phase, when the scientific investigation is mainly driven by the community.

2. The ASTRI Mini-Array

The ASTRI Mini-Array [13,14] consists of nine ASTRI dual-mirror small-sized (SSTs) Čerenkov telescopes, currently being deployed at the Observatorio del Teide (Spain), which will commence its scientific operations in late 2025. The ASTRI Mini-Array will provide a large field of view (FoV) of about 10°, a wide energy range from 1 TeV to 200 TeV, an angular resolution of $\sim 3'$, and an energy resolution of $\sim 10\,\%$. Table 1 compares the ASTRI Mini-Array performance with that of the current IACTs.

Table 1. Performance of the ASTRI Mini-Array compared with the main current IACT arrays. References: ASTRI Mini-array [15], MAGIC [16], VERITAS [17] and https://veritas.sao.arizona.edu (accessed on 14 February 2024), H.E.S.S. [2].

Quantity	ASTRI Mini-Array	MAGIC	VERITAS	H.E.S.S.
Location	28° 18′ 04″ N	28° 45′ 22″ N	31° 40′ 30″ N	23° 16′ 18″ S
	16° 30′ 38″ W	17° 53′ 30″ W	110° 57′ 7.8″ W	16° 30′ 00″ E
Altitude [m]	2390	2396	1268	1800
FoV	$\sim 10°$	$\sim 3.5°$	$\sim 3.5°$	$\sim 5°$
Angular Res.	0.05° (10 TeV)	0.07° (1 TeV)	0.07° (1 TeV)	0.06° (1 TeV)
Energy Res.	10% (10 TeV)	16% (1 TeV)	17% (1 TeV)	15% (1 TeV)
Energy Range	(0.5–200) TeV	(0.05–20) TeV	(0.08–30) TeV	(0.02–30) TeV [a]

Notes: [a]: considering the contribution of H.E.S.S.−−II telescope unit [18].

A detailed description of the ASTRI Mini-Array performance is reported in [19]. Figure 1 shows the ASTRI Mini-Array differential sensitivity (turquoise points, 50 h integration time, 5σ confidence level, C.L.) compared with those of the current major IACTs (H.E.S.S., MAGIC, and VERITAS) and of the planned CTAO. The ASTRI Mini-Array will improve the current IACT sensitivity at energies greater than a few TeVs and will be of the same order as that of CTAO North in the "alpha" (4 LSTs[2] + 9 MSTs[3] [9] configuration, and slightly better in the "science verification" (4 LSTs + 5 MSTs [20]) configuration, respectively, at energies greater than a few tens of TeVs.

The ASTRI Mini-Array will reserve, as we shall describe in Section 3, its first four years of operation for the investigation of a few specific science topics. This implies that most of the science operations will be performed as deep pointings, with exposures in the order of 200 h or even 500 h, towards specific sky regions. Figure 2 shows the ASTRI Mini-Array differential sensitivity curves for 200 h (turquoise squares) and 500 h (turquoise triangles) integration time, respectively. For such long integration times, the most appropriate comparison is with current EAS differential sensitivity curves, HAWC [21], Tibet AS-γ (Takita M., priv. comm. based on [22]), and LHAASO [23].

The main advantage of EAS with respect to IACTs is the former's 2 sr FoV and their larger duty cycle. On the other hand, as reported in Table 2, their energy and angular resolution in the same energy range as the ASTRI Mini-Array (about 10 TeV) are at least a factor of 3 to 4 times worse. Clearly, this makes the ASTRI Mini-Array extremely competitive in studying the morphology of extended sources and crowded fields and accurately monitoring multiple targets in the same pointing.
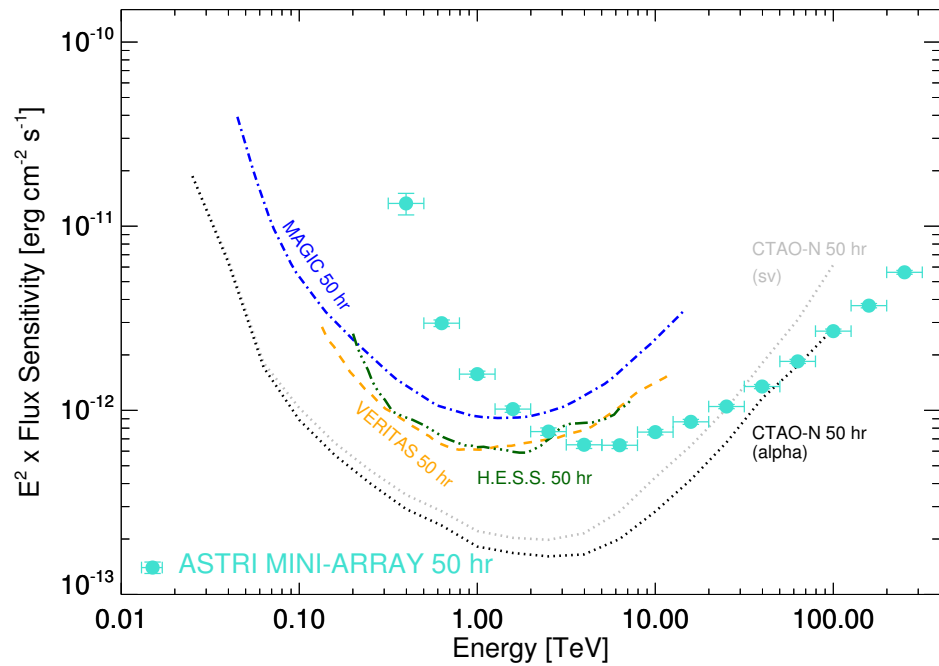
Figure 1. ASTRI Mini-Array differential sensitivity for 50 h integration compared with those of MAGIC, H.E.S.S., VERITAS, and CTAO North. The differential sensitivity curves are drawn from [19] (ASTRI Mini-Array), [16] (MAGIC), the VERITAS official website https://veritas.sao.arizona.edu (accessed on 14 February 2024), and [24] (sensitivity curve for H.E.S.S.−I, stereo reconstruction). CTAO−N "alpha configuration" (alpha) sensitivity curve comes from [9]. The CTAO−N "science verification" (sv) sensitivity is drawn from [20].
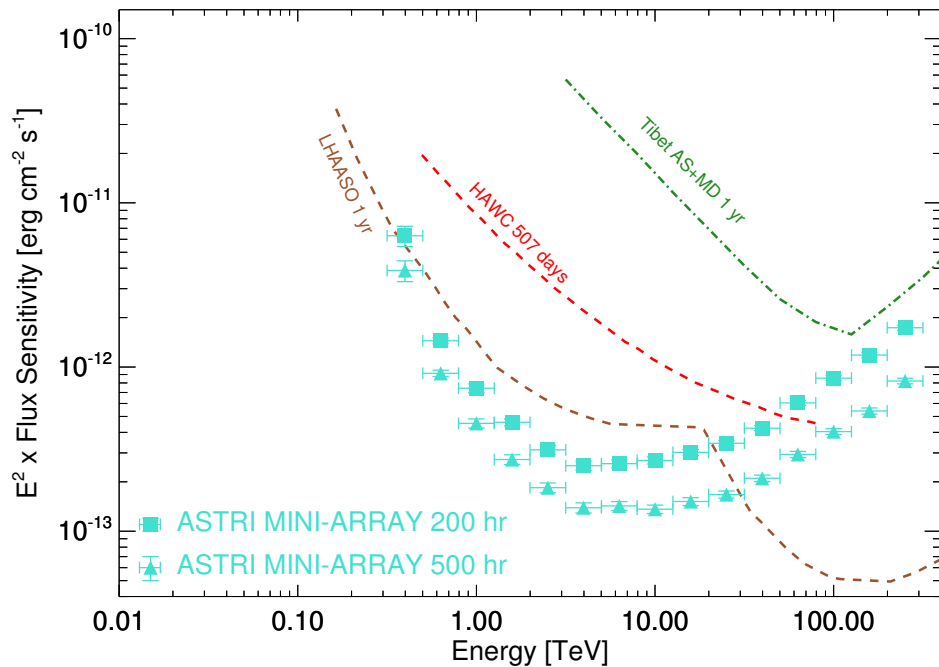
Figure 2. ASTRI Mini-Array differential sensitivity for 200 h (turquoise squares) and 500 h (turquoise triangles) integration times compared with those of HAWC (507 d), Tibet AS-γ (1 yr), and LHAASO (1 yr). The differential sensitivity curves are drawn from ASTRI Mini-Array [19], HAWC [21], LHAASO [23], and Takita M. (priv. comm.) based on [22] (Tibet AS + MD). We note that the 507-day HAWC differential sensitivity curve corresponds to about 3000 h of acquisition on a source at a declination of 22° within its field of view [21].

Table 2. Summary of the performance of the current main particle sampling arrays compared with those of the ASTRI Mini-Array. References: ASTRI Mini-array [15], HAWC [5,25], LHAASO [6], Tibet AS-γ [22,26].

Quantity	ASTRI Mini-Array	HAWC	LHAASO	Tibet AS-γ
Location	28° 18′ 04″ N 16° 30′ 38″ W	18° 59′ 41″ N 97° 18′ 27″ W	29° 21′ 31″ N 100° 08′ 15″ E	30° 05′ 00″ N 90° 33′ 00″ E
Altitude [m]	2390	4100	4410	4300
FoV	∼0.024 sr	2 sr	2 sr	2 sr
Angular Res.	0.05° (10 TeV)	0.15° [a] (10 TeV)	(0.24–0.32)° [b] (100 TeV)	0.2° [c] (100 TeV)
Energy Res.	10% (10 TeV)	30% (10 TeV)	(13–36)% (100 TeV) [b]	20% [c] (100 TeV)
Energy Range	(0.5–200) TeV	(0.1–1000) TeV	(0.1–1000) TeV	(0.1–1000) TeV

Notes: [a]: (0.15–1)° as a function of the event size. [b]: angular resolution is (0.70–0.94)° at 10 TeV; (0.24–0.32)° at 100 TeV; 0.15° at 1000 TeV. Energy resolution is (30–45)% at 10 TeV; (13–36)% at 100 TeV; (8–20)% at 1000 TeV [27]. [c]: angular resolution is ∼ 0.5° at 10 TeV and ∼0.2° at 10 TeV at 50% containment radius [22]. Energy resolution is ∼40% at 10 TeV and ∼20% at 100 TeV [26]. The different values of the LHAASO angular and energy resolution performance at a given energy have been computed at different Zenith angles, $0 < \theta < 20$, $20 < \theta < 35$, and $35 < \theta < 50$ degrees, respectively. At lower Zenith angles, the performance is better.

Furthermore, the ASTRI Mini-Array angular resolution will allow us to investigate the LHAASO uncertainty error box of Galactic sources, which is of the order of one degree [28] and study the different sources possibly associated with the PeV emission, in order to unambiguously identify them, when in synergy with GeV and X-ray facilities.

Figure 3 shows the ASTRI Mini-Array angular (left panel) and energy (right panel) resolution as a function of the energy as reported in [19].
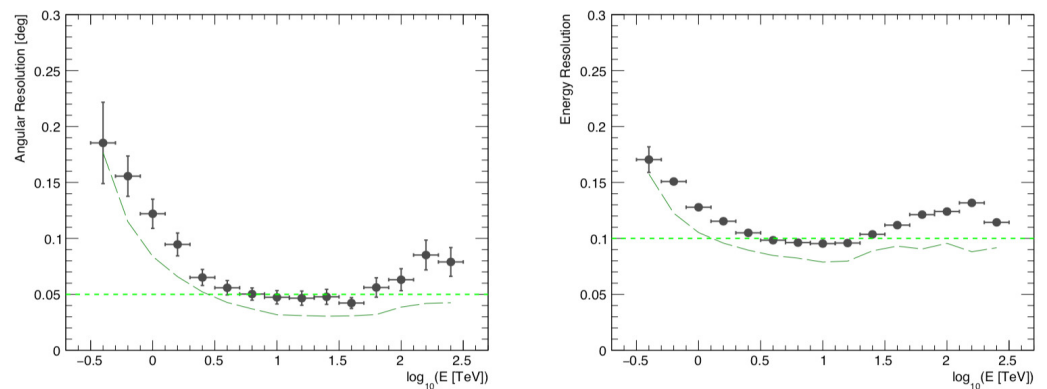
Figure 3. ASTRI Mini-Array angular (**left panel**) and energy (**right panel**) resolution as a function of the energy. The angular resolution is defined as the 68% γ-ray event containment radius (in degrees). The black points were computed with analysis cuts optimizing the differential sensitivity in 50 h; the long-dashed, dark-green lines were instead derived with analysis cuts taking into account also the angular/energy resolution in the optimization; the short-dashed, light-green lines mark the 0.05° and the 0.1% threshold for the angular and energy resolution, respectively. Adapted from [19].

3. Core Science Topics

The ASTRI Mini-Array science program will develop in two phases. During the first four years of operations, the ASTRI Mini-Array will be run as an *experiment*, while in the subsequent four years, it will gradually evolve into an *observatory* open to the scientific community.

A graphical description of the main Core Science topics that we plan to investigate during the first four years of operations is shown in Figure 4. Our Core Science Program is based on "Main Pillars". They are science fields in which the ASTRI Mini-Array will

contribute breakthrough pieces of evidence to improve our understanding of a few key science questions.
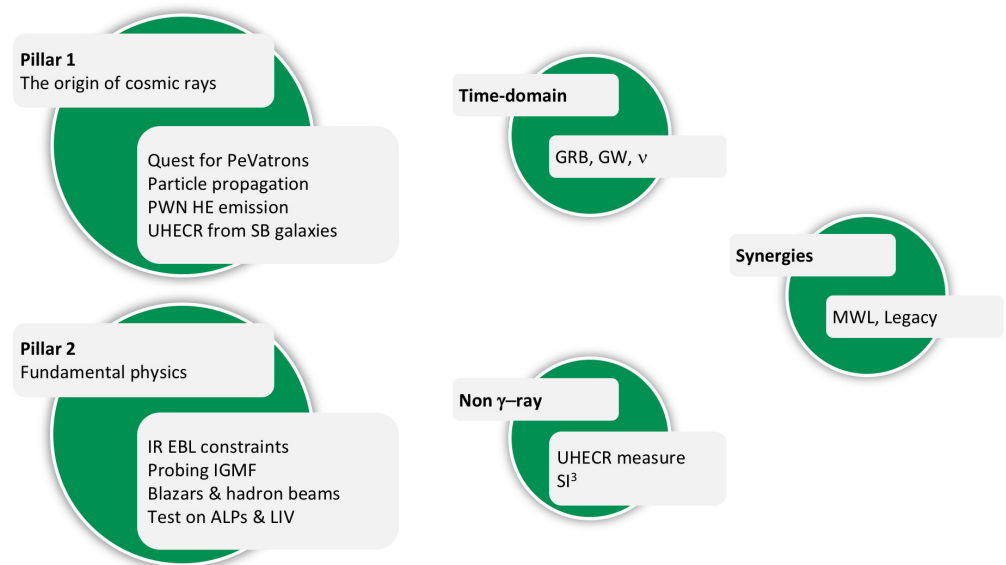
Figure 4. Graphical description of the ASTRI Mini-Array Core Science program.

Recently, [15] discussed the ASTRI Mini-Array Core Science, which includes the study of the: (1) origin of cosmic rays; (2) cosmology and fundamental physics; (3) GRBs and time-domain astrophysics; (4) direct measurements of cosmic rays; (5) stellar-intensity interferometry. Here, I will review some of the results on all science topics, while Section 4.1 will focus on the Observatory Science ones, presented in [29,30].

3.1. The Origin of Cosmic Rays

The LHAASO Collaboration [28] reported the discovery of twelve Galactic sources emitting γ-rays at several hundreds TeV up to 1.4 PeV. These sources are able to accelerate particles up to $\sim 10^{15}$ eV, making them "PeVatron candidates". We note that the majority of these sources are diffuse γ-ray structures with angular extensions up to 1°, which, together with the LHAASO limited angular resolution, make the identification of the actual sources responsible for the ultra high-energy γ-ray emission not univocal (except for the Crab Nebula). The recent publication of the First LHAASO Catalog of γ-ray Sources (1LHHASO [31]) containing 90 sources, 43 of them with emissions at energies $E > 0.1$ PeV, marks a fundamental step for the astrophysics at very high- and ultra high-energies. This discovery is extremely important for the ASTRI Mini-Array science, especially because of its angular resolution, which, at energies of about 100 TeV, is a factor of 3 to 4 times better in radius than the LHAASO one: 0.08° vs. 0.24–0.32°. We should also mention that both the angular resolution and the energy resolution can be improved by means of specific analysis cuts, as shown in Figure 3. The ASTRI Mini-Array will investigate these and future PeVatron sources, providing important information on their morphology above 10 TeV. The ASTRI Mini-Array wide FoV will be extremely important in the investigation of extended regions and point-like sources. A single pointing will allow us to investigate the Galactic Center or the Cygnus regions. In these regions, we can accumulate several hundreds of hours by also including the epochs of moderate Moon condition [32]. This is crucial to investigate both the (energy-dependent) morphology of the sources in these regions and their possible variability on a long time scale. The ASTRI Mini-Array will investigate the Galactic Center at a high Zenith angle (maximum culmination angle of $\sim 57°$). We expect to be able to study this region up to $E \sim 200$ TeV for an exposure time of 260 h, significantly improving the current results of other IACTs (see for further details [15]). The high-energy boundaries of the ASTRI Mini-Array will also be important to study the

Crab Nebula, the only Galactic PeVatron[4] currently known [33,34]. The origin of the Crab Nebula γ-ray emission detected by LHAASO does not require a hadronic contribution but cannot exclude it either. A deep ASTRI Mini-Array observation lasting about 500 h in the $E > 100$ TeV energy range should definitely be able to provide constraints on the proton component in this source.

3.2. Cosmology and Fundamental Physics

IACT arrays detected extra-galactic sources since the early nineties [35]. Since then, among the 280 sources listed in TeVCat, 93 are found to be extra-galactic: 55 high-peaked BL Lacs (HBLs), 10 intermediate-peaked BL Lacs (IBLs), 9 flat-spectrum radio quasars (FSRQs), 4 Blazars, 4 Fanaroff-Riley Type (FR-I) galaxies, 2 star-bursting galaxies (SBGs), 2 BL Lacertae objects with class unclear (BL Lacs), 2 unknown type AGNs, and 5 γ-ray bursts (GRBs). Extra-galactic jetted sources are excellent probes for several science cases. They can be used to investigate the extra-galactic background light, as well as to probe, by means of variability studies, the properties of the γ-ray emitting region. They can also be useful to investigate peculiar physical phenomena, such as the existence of the axion-like particle, to test the Lorentz invariance violation, and to study the intergalactic magnetic fields.

THE EXTRA-GALACTIC BACKGROUND LIGHT (EBL)—The EBL significantly affects the spectra of jetted sources at energies that can be explored by the ASTRI Mini-Array. Moreover, the EBL direct measurement in the infra-red (IR) portion of the spectrum is particularly challenging because of the dominant contribution of our Galaxy at these wavelengths. Nevertheless, the ASTRI Mini-Array can contribute to the study of the EBL IR component given the well-known relation $\lambda_{\mathrm{max}} \simeq 1.24 \times E_{\mathrm{TeV}}$ µm, between the wavelength of the target EBL photon, λ_{max} and the energy of the γ-ray, E_{TeV}. The IR component in the $(10 < \lambda < 100)$ µm regime represents a challenge because of the dominance of local emission from both the Galaxy and our Solar system. The preferred candidates for observations with the ASTRI Mini-Array are TeV-emitting low-redshift radio-galaxies and local star-bursting galaxies. Among the sources fulfilling these criteria, we investigated the low-redshift radio-galaxies IC 310 ($z{\sim}0.0189$) and M 87 ($z{\sim}0.00428$). For IC 310 we assumed three different spectral states: flare [36], high and low [37]. Short (5 h) and deep (200 h) observations will allow us to detect these sources in different spectral states at energies $E > 10$ TeV, thus probing the IR EBL component. Similar results can be obtained for M 87 in different spectral states, as reported by [38] (low state), [39] (high state), and [40] (flaring state).

FUNDAMENTAL AND EXOTIC PHYSICS—Blazar spectra above a few TeV are excellent probes of non-standard γ-ray propagation effects such as the presence of hadron beams (HB) in the jet of extreme BL Lac objects (E-HBL and references therein [41]), the existence of axion-like particles [42] (ALP), or the effects of the Lorentz invariance violation (LIV and references therein [41]) and the properties of inter-galactic magnetic fields (IGMF and references therein [43]). The most promising sources to detect spectral signatures induced by these effects are 1ES 0229+200 (E-HBL, $z{\sim}0.139$) and Mrk 501 (HBL, $z{\sim}0.03298$). The presence of HB implies that the spectrum of blazars extends at energies above those allowed by the standard EBL model [44]. A detection of a γ-ray photons at energies of a few tens of TeV, when the standard EBL model would imply a roll-off at a few TeV, could be the signature for the presence of the HB scenario. On the other hand, this excess at energies above a few tens of TeV could also be induced by both the ALPs and LIV effects. ALPs produce a distinctive oscillation pattern in the blazar spectrum, that could represent the unique marker for this process, but it would require a much finer energy resolution than that of the ASTRI Mini-Array to be revealed. Also, in the context of the widely studied dark matter (DM) weakly-interacting massive particles scenario, the ASTRI Mini-Array may provide interesting DM-related insights from dwarf spheroidal galaxies and Galactic center observations, particularly for the case of monochromatic γ-ray emission lines [30]. In order to address all these studies we can plan deep (in the order of 200 h) dedicated pointing,

a typical exposure that could be accumulated during the first years, with the described ASTRI Mini-Array observing strategy.

3.3. Multi-Messenger and Time-Domain Astrophysics

Transients and multi-messenger studies such as γ-ray bursts (GRBs), gravitational waves (GWs), and neutrino emission (ν_s) from VHE sources are indeed the new frontiers of high-energy astrophysics.

γ-RAY BURSTS—GRBs have only been detected by IACTs starting from 2018 and, at the time of writing, we only count six[5] GRBs detected at energies in excess of 0.1 TeV: GRB 160821B ($z = 0.162$, MAGIC] [45]), GRB 180720B ($z = 0.653$, H.E.S.S. [46]), GRB 190114C ($z = 0.424$, MAGIC [47]), GRB 190829A ($z = 0.078$, H.E.S.S. [48]), GRB 201015A ($z = 0.42$, MAGIC [49]), GRB 201216C ($z = 1.1$, MAGIC [50]), GRB 221009A ($z = 0.151$, LHAASO] [51]). Two of them are particularly relevant for the ASTRI Mini-Array. GRB 190114C is the first GRB detected at VHE within one minute from the T_0, up to an energy of about 1 TeV. GRB 221009A, described as *"to be a once-in-10,000-year event"* [52,53] was detected by LHAASO up to 13 TeV [54], challenging the standard emission scenario for the canonical EBL absorption [55,56]. Taking into account the energetics observed in GRB 221009A, we can estimate that this event, placed at a different redshift ($z = 0.078, 0.25, 0.42$), can be detected up and above 10 TeV by the ASTRI Mini-Array within a few minutes from the event (L. Nava, Priv. Comm.).

NEUTRINOS—AGNs can be sources of extra-galactic ν_s. The IceCube data [57] seem to indicate that there could be an association between ν_s emission and a few AGNs: a Seyfert-2 galaxy (NGC 1068, $D = 14.4$ Mpc), and two BL Lac objects (TXS 0506 + 056, $z = 0.3365$; PKS 1424 + 240, $z = 0.16$). Although the two latter sources are known TeV emitters, NGC 1068 shows prominent emission only in the 0.1–300 GeV energy band [58,59]. NGC 1068 could show emission above 10 TeV under the assumption of a dominant contribution of relativistic particles accelerated by the AGN-driven wind, as discussed in Section 4.4.

3.4. Non γ-ray Astrophysics

STELLAR INTENSITY INTERFEROMETRY—Stellar intensity interferometry (SII) is based on the second-order coherence of light, which allows imaging sources at the level of 100 μas. This means that it is possible to reveal details on the surface and of the environment surrounding bright stars in the sky, which typically have angular diameters of 1–10 mas. The SII observing mode will take advantage of an additional, dedicated instrument that is being designed and will be installed on the ASTRI Mini-Array telescopes [60].

DIRECT MEASUREMENTS OF COSMIC RAYS—More than 99% of the signal acquired by the ASTRI Mini-Array is hadronic in nature. In particular, this hadronic component could be useful to investigate the cosmic ray composition in the TeV–PeV energy range and the measurement of the cosmic ray spectrum at energies characteristics of its "knee".

3.5. Synergies with Other Facilities

The ASTRI Mini-Array will be operating during a period when several facilities will cover the whole electromagnetic spectrum, from radio to PeV. The Sardinia radio telescope (SRT) will complement VHE observation with radio data at different frequencies, both for Galactic and extra-galactic objects. Galactic sources already observed with SRT are W 44, IC 433, and Tycho [61,62]. In the optical energy band, the Telescopio Nazionale Galileo [63] and the GASP/WEBT Consortium [64] can provide excellent coverage, as well as several facilities managed by Instituto de Astrofísica de Canarias (IAC) at the Canary Island. In the X-ray energy band, in addition to the long-standing ESA and NASA legacy Observatories, we can now exploit the eROSITA [65] surveys and, in particular, the IXPE [66] X-ray polarimetric data. At the extreme energy boundary, LHAASO, HAWC, and Tibet AS-γ will extend data at energies of a few PeV.

The ASTRI Mini-Array location at the Observatorio del Teide and its collaboration with the IAC will allow us to investigate sources synergically with both the MAGIC and CTAO−N arrays. In particular, they will be of paramount importance for their capability to investigate not only the local Universe but also to reach redshifts well beyond one and perform cosmological studies on extra-galactic sources. Moreover, both MAGIC and CTAO−N will allow us to extend the ASTRI Mini-Array spectral performance in the sub-TeV regime, with almost no breaks from a few tens of GeV up to hundreds of TeV.

4. The Observatory Phase

The ASTRI Mini-Array science program will gradually evolve from an experiment towards an Observatory Phase, built on the experience and results from the Core Science phase, and open to observational proposals from the scientific community at large. We foresee important synergies with the above-mentioned facilities to yield the best scientific return from the proposed observations.

An example of such synergies is illustrated in Figure 5, where we show, in Galactic coordinates and Aitoff projection, the First LHAASO Catalog of γ-ray Sources (1LHHASO, [31]) plotted as orange dots and, superimposed, the ASTRI Mini-Array Core Science target regions for both Pillar-1 (blue circles) and Pillar-2 (red circles) targets. Some 1LHAASO sources already overlap the ASTRI Mini-Array selected Pillar regions, in particular along the Galactic Plane. We also note that Mrk 501 and Mrk 421 are natural candidates for common variability studies.
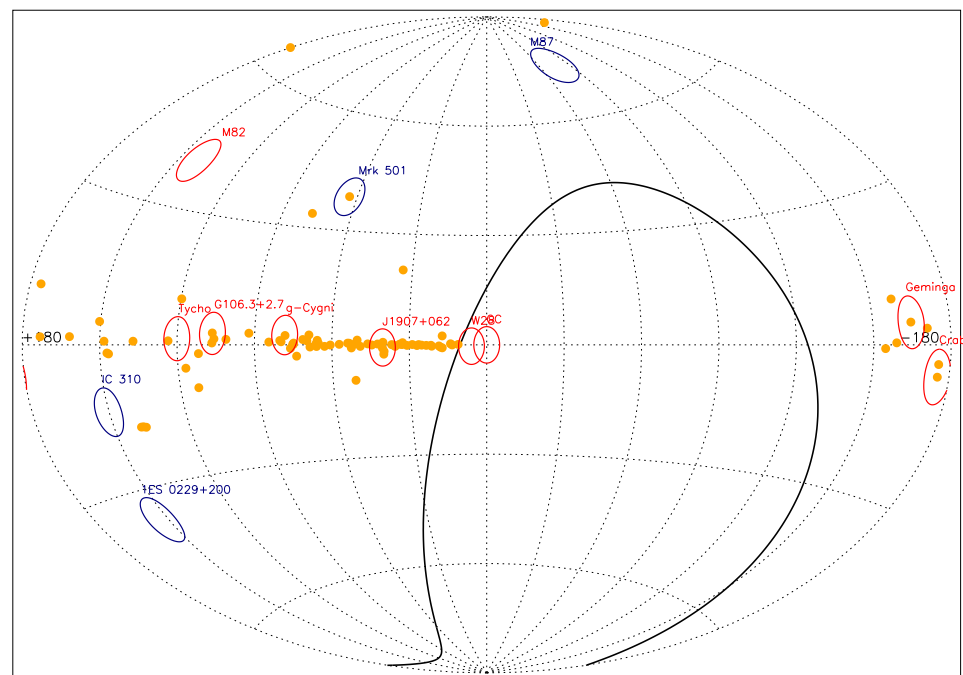
Figure 5. Pillar-1 and Pillar-2 target regions (red and blue circles, $\approx 10°$ in diameter) and 1LHAASO sources (orange dots) on the sky in Galactic coordinates (Aitoff projection). The black solid line shows the declination limit for the ASTRI Mini-Array pointings.

We can now discuss a few examples of foreseeable investigations that can be performed during the Observatory Phase. Since this phase will be open to the scientific community through competitive proposals, these examples represent ideas on how to best employ the ASTRI Mini-Array capabilities.

4.1. Cygnus Region Mini-Survey

The ASTRI Mini-Array wide FoV is well suited to perform mini-surveys of selected sky regions. One of the most important ones, as shown in Figure 5, is the Cygnus Region

$(60° < l < 90°)$, which contains several sources emitting above a few TeV, as reported in the First LHAASO Catalog. Figure 6 shows the results of a possible ASTRI Mini-Array mini-survey of this region with different exposure times, 50 h, 100 h, and 200 h from top to bottom, respectively.
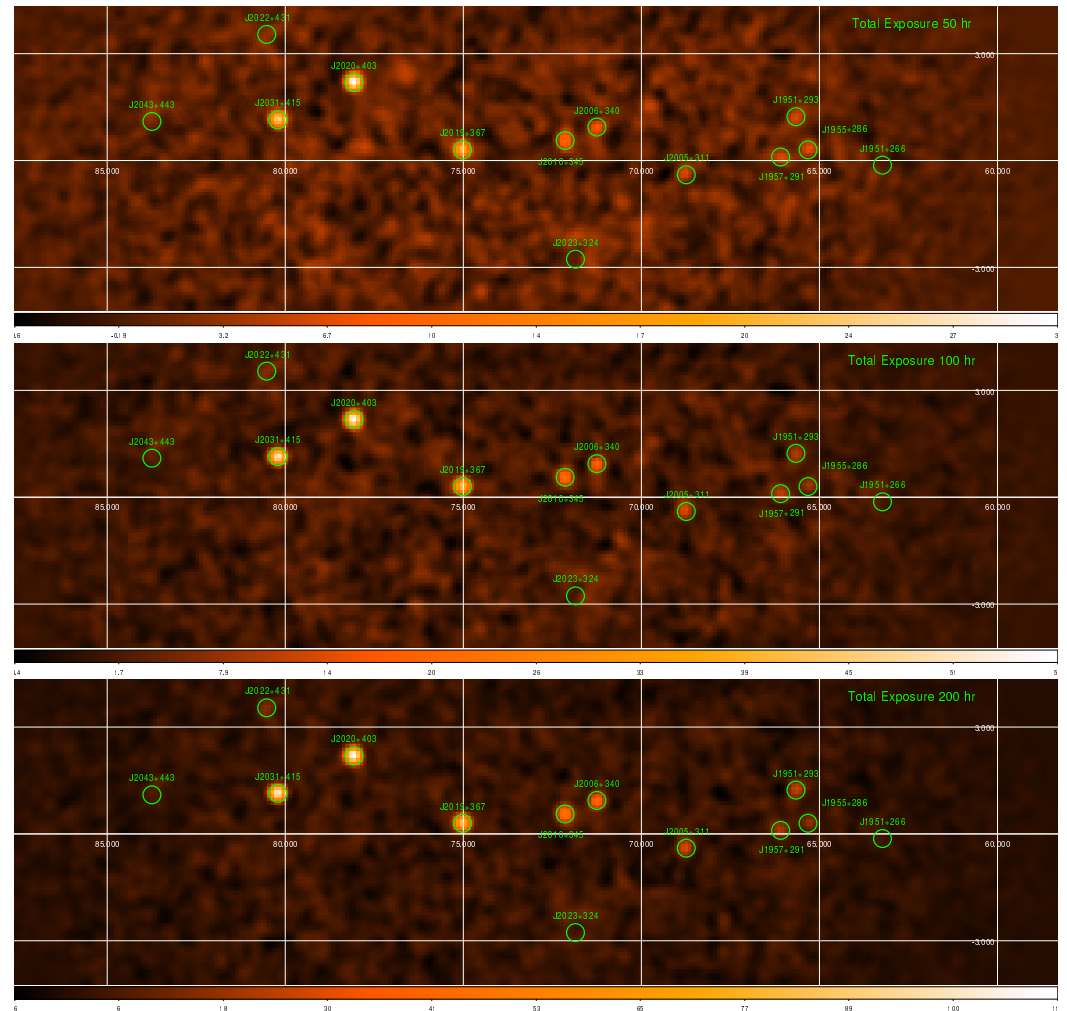
Figure 6. ASTRI Mini-Array simulations of the Cygnus region mini-survey. The count maps were produced assuming for each pointing an exposure of 1 h (**top panel**), 2 h (**middle panel**), and 4 h (**bottom panel**), respectively. Sky map units are counts/pixels. From [29].

The simulations, discussed in [29], combined fifty different pointings, at the same Galactic latitude and spaced by 0.4° in Galactic longitude, from $(l, b) = (64, 0)$ to $(l, b) = (84, 0)$, and lasting 1 h, 2 h, and 4 h hours each, respectively. The very high-energy simulated sources were drawn from the Third HAWC Catalog of very high-energy γ-ray sources (3HWC [67]). Thirteen of them fall inside the area considered and were simulated according to their published spectral parameters. Ten of these very high-energy sources are always significantly detected by the ASTRI Mini-Array, even at the shortest (50 h) exposure time. Recently, [68] reported the detection of an extend (about 6° in diameter) γ-ray emission centered on Cygnus-X $(l,b) \approx (80°, 0°)$ with 66 photon-like events with energies greater than 400 TeV (see Figure 1 in [68]). The ASTRI Mini-Array wide FoV ($\sim 10°$ in diameter) and the stable off-axis performance (see Section 2) will allow us to investigate this region with a single pointing and prolonged exposure, performing a more accurate morphological measurement on the core region of the bubble discovered by LHAASO.

4.2. Gamma-Ray Binaries—LS 5039

A recent study [69] discusses the properties of γ-ray binaries. We currently know ten non-transient γ-ray binaries: seven have a compact source (six are located in our Galaxy and one, LMC P3, in the Large Magellanic Cloud), while three are colliding-wind binaries. We discuss the results of ASTRI Mini-Array simulations of LS 5039 to show the ASTRI Mini-Array capabilities of reproducing both the folded light-curve and the spectrum in different orbital phases for this source. We simulated 300 h of total exposure, 250 h in the low state, and 50 h in the high state (see [70] for a detailed description of the different flux levels). The orbit-averaged spectrum[6], described in [71], is a cut-off power-law with $\Gamma = 2.06 \pm 0.05$ and $E_{\mathrm{cut}} = 13.0 \pm 4.1$ TeV. We simulated a fixed exposure time of 10 h for each phase bin. Figure 7 shows the simulation results, the flux (left panel), and the $1\,\sigma$ uncertainty ($\delta\Gamma$) on the spectral index (right panel) as a function of the orbital phase. The simulated source flux is fully consistent with the flux expected from the model. Moreover, for 90% of the orbital phase, the uncertainty on the photon index, $\delta\Gamma$, is between 0.1 and 0.25, while only in the case of the lowest-flux bin (phase range 0.1–0.2) its value rises up to about 0.4.
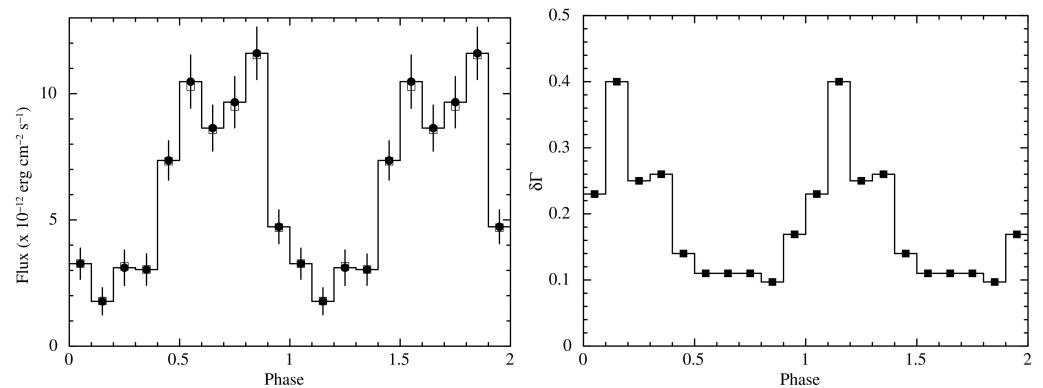
Figure 7. ASTRI Mini-Array simulations of LS 5039. **Left panel**: orbital modulation obtained with 10 h-long simulations per orbital phase bin. The open squares are the expected fluxes from the models, while the filled circles are the simulated fluxes in 0.8–200 TeV. Error bars are at $1\,\sigma$ C.L. **Right panel**: $1\,\sigma$ uncertainty ($\delta\Gamma$) on the spectral index obtained for 10 h-long simulations per orbital bin. From [29].

4.3. Spectral Features—Mrk 501

Mrk 501 ($z = 0.032983 \pm 0.00005$) is the second extra-galactic source detected at VHE [72]. It is classified as a high-synchrotron-peaked BL Lac object, which means that the synchrotron peak of the usual double-humped blazar spectral energy distribution reaches the ultra-violet energy band or even higher frequencies ($\nu_{\mathrm{peak}} \gtrsim 10^{15}$ Hz). This source is extremely variable, at almost all frequencies. Recently MAGIC detected a peculiar spectral feature during the highest X-ray ($E > 0.3$ KeV) flux ever recorded from this source [73].

The spectral feature, emerging during the highest X-ray flux state at about 3 TeV with a significance of $\approx 4\sigma$, can be modeled both as a curved narrow-band log-parabola or a Gaussian function superimposed to a broad-band simple log-parabola, respectively. The physical interpretation is still debated and three possible scenarios can be invoked: a two-zone emitting region model, a pile-up in the electron energy distribution, or a pair cascade from electrons accelerated in a black hole magnetospheric vacuum gap. Figure 8 shows the ASTRI Mini-Array simulations performed to investigate its capabilities in terms of energy resolution to detect such spectral features. Simulations (see [30] for a detailed discussion) were performed to investigate the percentage of number of detections of the spectral feature with respect to a broad-band log-parabola above 5σ confidence level for 200 realizations. In order to have at least a $\approx 50\%$ probability of detection of the feature, 1.5 h of observation time would be required, increasing up to $\approx 80\%$ probability for 2 h of exposure.
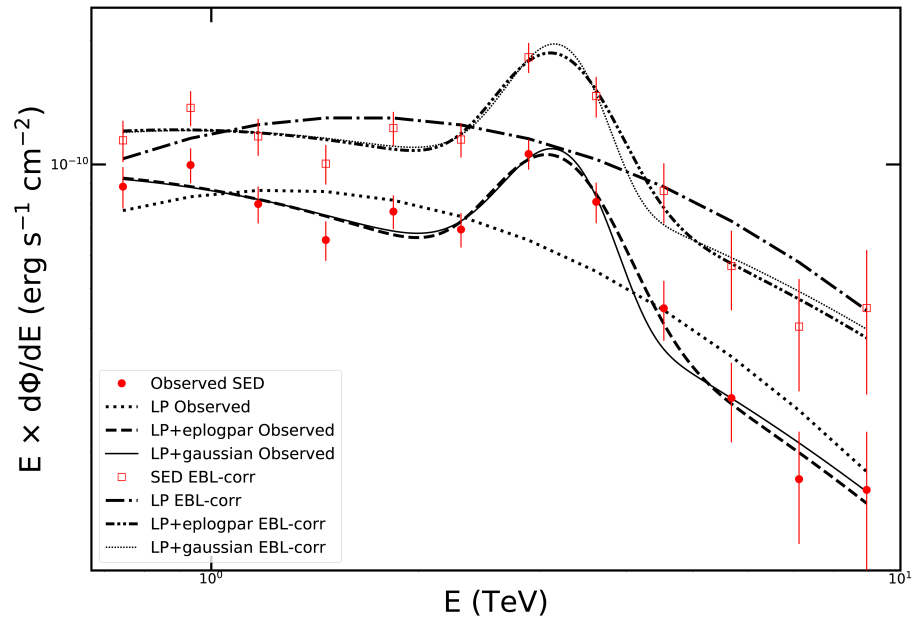
Figure 8. ASTRI Mini-Array simulations of the spectral feature emerging at ≈3 TeV in the spectrum on Mrk 501 during its highest ever-recorded X-ray flux state. LP = log-parabola; eplogpar = curved log-parabola; EBL = extra-galactic background light. From [30].

4.4. Disentangling Spectral Models in Misaligned Jetted Sources—NGC 1068

NGC 1068 ($z = 0.00379 \pm 0.00001$) is a powerful γ-ray Seyfert-2 galaxy detected by *Fermi*-LAT. It also hosts starburst activity in its central region and AGN-driven winds. The origin of the γ-ray emission is still debated because of the presence of different particle acceleration sites, such as the starburst ring, the circum-nuclear disk, and the jet [58,74]. Moreover, it has recently been associated with a possible source of neutrino emission [57]. While the canonical jet model does not extend above 10 TeV (see [74]), the AGN wind model predicts a hard spectrum that extends in the very high energy band. Figure 9 shows the results of a simulated deep observation (200 h) to test if we can detect VHE emission expected by the AGN wind model. The ASTRI Mini-Array is able to measure the source spectrum in the energy bins ∼2–5 TeV and ∼5–13 TeV at about 5 σ level.
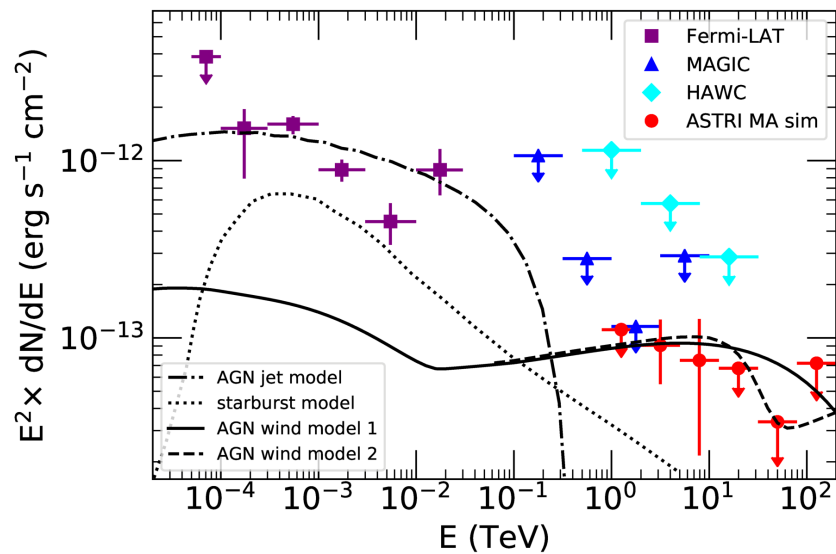
Figure 9. ASTRI Mini-Array simulations of the NGC 1068 VHE spectral energy distribution. Different emission models (see [74] for a detailed description) have been considered. From [30].

5. Conclusions

The ASTRI Mini-Array will commence scientific observations at the end of 2025 from the Observatorio del Teide, collecting data that will create a natural connection between current and future VHE facilities and other multi-wavelength observatories by providing light-curves, spectra, and high-resolution images of point-like and extended sources. Its 10° field of view will allow us to investigate both extended sources (e.g., supernova remnants) and crowded/rich fields (e.g., the Galactic Center) with a single pointing, while its 3' angular resolution at 10 TeV will allow us to perform detailed morphological studies of extended sources. Moreover, its sensitivity, extending above 100 TeV with a moderate degradation (about a factor of 2) up to the edge of the FoV, will make it the most sensitive IACT in the 5–200 TeV energy range in the Northern Hemisphere before the advent of CTAO−N. The ASTRI Mini-Array will join the energy domain typical of EASs with the precision domain (excellent angular and energy resolutions) typical of IACTs, allowing several synergies with LHAASO, HAWC, and Tibet AS-γ, investigating PeV-only sources, obtaining broad-band spectra, and detailed source morphology. For the first four years, the ASTRI Mini-Array will be run as an experiment with dedicated pointings in order to address specific Core Science Topics. Afterward, we expect a smooth transition toward an Observatory Phase open to observational proposals from the scientific community.

Funding: This work received no funding.

Data Availability Statement: This research has made use of the ASTRI Mini-Array Instrument Response Functions (IRFs) provided by the ASTRI Project [75] which are publicly available. All physical models are available through the cited literature. The ASTRI Mini-Array simulations were performed using the publicly available software `ctools` [v1.6.3] [76] and `gammapy` [v0.17] [77].

Acknowledgments: This work was conducted in the context of the ASTRI Project thanks to the support of the Italian Ministry of University and Research (MUR) as well as the Ministry for Economic Development (MISE), with funds explicitly assigned to the Italian National Institute of Astrophysics (INAF). We acknowledge the support of the Brazilian Funding Agency FAPESP (Grant 2013/10559-5) and the South African Department of Science and Technology through Funding Agreement 0227/2014 for the South African Gamma-Ray Astronomy Program. IAC is supported by the Spanish Ministry of Science and Innovation (MICIU). They are partially supported by H2020-ASTERICS, a project funded by the European Commission Framework Programme Horizon 2020 Research and Innovation action under grant agreement n. 653477. The ASTRI project is becoming a reality thanks to Giovanni "Nanni" Bignami, Nicolò "Nichi" D'Amico, two outstanding scientists who, in their capability as INAF Presidents, provided continuous support and invaluable guidance. Although Nanni was instrumental in starting the ASTRI telescope, Nichi transformed it into the Mini-Array in Tenerife. Now, the project is being built owing to the unfaltering support of Marco Tavani, the current INAF President. Paolo Vettolani and Filippo Zerbi, the past and current INAF Science Directors, and Massimo Cappi, the Coordinator of the High Energy branch of INAF, have been also very supportive of our work. We are very grateful to all of them. Unfortunately, Nanni and Nichi passed away, but their vision still guides us. This review went through the internal ASTRI review process. SV also wishes to thank the *Universe* Editor of the Special Issue "Recent Advances in Gamma Ray Astrophysics and Future Perspectives", P. Romano, for inviting him to write a review, and the referees for their comments that helped improve the manuscript.

Conflicts of Interest: The author declares no conflict of interest.

Abbreviations

The following abbreviations are used in this manuscript:

ALP	Axion-like particles
AS-γ	Air shower γ-ray array
ASTRI	Astrofisica con specchi a tecnologia replicante italiana
C.L.	Confidence Limit
CTAO	Čerenkov telescope array Observatory
DM	Dark matter

EAS	Extended air showers arrays
ESA	European space agency
EBL	Extra-galactic background light
E-HBL	Extreme high-peaked BL Lacs
eROSITA	Extended Roentgen survey with an imaging telescope array
FOV	Field of view
FR	Fanaroff–Riley galaxies
FSRQ	Flat-spectrum radio quasar
GASP	GLAST-AGILE support programme
GRB	Gamma-ray burst
GW	Gravitational wave
HAWC	High-altitude water Čerenkov observatory
HB	Hadron Beam
HBL	High-peaked BL Lacs
HE	High-energy
H.E.S.S.	High-energy stereoscopic system
IAC	Instituto de Astrofísica de Canarias
IACT	Imaging atmospheric Čerenkov telescope arrays
IBL	Intermediate-peaked BL Lacs
IGMF	Inter-galactic magnetic field
IR	Infra-red
IXPE	Imaging X-ray polarimetry explorer
LHAASO	Large high-altitude air shower observatory
LIV	Lorentz invariance violation
LST	Large-sized telescope
MAGIC	Major atmospheric gamma-ray imaging Čerenkov telescopes
MST	Medium-sized telescope
NASA	National aeronautics and space administration
SBG	Star-bursting galaxies
SC	Schwarzschild-Couder
SII	Stellar intensity interferometry
SRT	Sardinia radio telescope
SST	Small-sized telescope
TNG	Telescopio Nazionale Galileo
VERITAS	Very energetic radiation imaging telescope array system
VHE	Very high-energy
WEBT	Whole-Earth blazar telescope

Notes

1. http://tevcat.uchicago.edu/, accessed on 14 February 2024.
2. Large-sized telescopes.
3. Medium-sized telescopes.
4. As noted in [33], a 1.1 PeV photon requires a parent electron of energy $E \sim 2.3$ PeV.
5. GRB 160821B and GRB 201015A have been detected at a significance of $\sim 3.1\,\sigma$ and $\sim 3.5\,\sigma$, respectively, contrary to all the other GRBs whose detection significance exceeds $\sim 5\,\sigma$.
6. More detailed, phase-resolved spectra could not be investigated given the short exposure times in each phase bin.

References

1. Wakely, S.P.; Horan, D. TeVCat: An online catalog for Very High Energy Gamma-Ray Astronomy. *Int. Cosm. Ray Conf.* **2008**, *3*, 1341–1344.
2. Aharonian, F.; Akhperjanian, A.G.; Bazer-Bachi, A.R.; Beilicke, M.; Benbow, W.; Berge, D.; Bernlöhr, K.; Boisson, C.; Bolz, O.; Borrel, V.; et al. Observations of the Crab nebula with HESS. *A&A* **2006**, *457*, 899–915. [CrossRef]
3. Aleksić, J.; Alvarez, E.A.; Antonelli, L.A.; Antoranz, P.; Asensio, M.; Backes, M.; Barrio, J.A.; Bastieri, D.; Becerra González, J.; Bednarek, W.; et al. Performance of the MAGIC stereo system obtained with Crab Nebula data. *Astropart. Phys.* **2012**, *35*, 435–448. [CrossRef]
4. Weekes, T.C.; Badran, H.; Biller, S.D.; Bond, I.; Bradbury, S.; Buckley, J.; Carter-Lewis, D.; Catanese, M.; Criswell, S.; Cui, W.; et al. VERITAS: The Very Energetic Radiation Imaging Telescope Array System. *Astropart. Phys.* **2002**, *17*, 221–243. [CrossRef]

5. Abeysekara, A.U.; Albert, A.; Alfaro, R.; Alvarez, C.; Álvarez, J.D.; Arceo, R.; Arteaga-Velázquez, J.C.; Ayala Solares, H.A.; Barber, A.S.; Bautista-Elivar, N.; et al. Observation of the Crab Nebula with the HAWC Gamma-Ray Observatory. *Astrophys. J.* **2017**, *843*, 39. [CrossRef]

6. Cao, Z. A future project at tibet: The large high altitude air shower observatory (LHAASO). *Chin. Phys. C* **2010**, *34*, 249–252. [CrossRef]

7. Amenomori, M.; Bi, X.J.; Chen, D.; Chen, T.L.; Chen, W.Y.; Cui, S.W.; Danzenguluobu; Ding, L.K.; Feng, C.F.; Feng, Z.; et al. Search for Gamma Rays above 100 TeV from the Crab Nebula with the Tibet Air Shower Array and the 100 m^2 muon Detector. *Astrophys. J.* **2015**, *813*, 98. [CrossRef]

8. Cherenkov Telescope Array Consortium; Acharya, B.S.; Agudo, I.; Al Samarai, I.; Alfaro, R.; Alfaro, J.; Alispach, C.; Alves Batista, R.; Amans, J.P.; Amato, E.; et al. *Science with the Cherenkov Telescope Array*; World Scientific: Singapore, 2019. [CrossRef]

9. Gueta, O. The Cherenkov Telescope Array: Layout, design and performance. In Proceedings of the 37th International Cosmic Ray Conference, Virtual, 12–23 July 2022; p. 885. [CrossRef]

10. Scuderi, S. The ASTRI Program. *Eur. Phys. J. Web Conf.* **2019**, *209*, 01001. [CrossRef]

11. Giro, E.; Canestrari, R.; Sironi, G.; Antolini, E.; Conconi, P.; Fermino, C.E.; Gargano, C.; Rodeghiero, G.; Russo, F.; Scuderi, S.; et al. First optical validation of a Schwarzschild Couder telescope: The ASTRI SST-2M Cherenkov telescope. *A&A* **2017**, *608*, A86. [CrossRef]

12. Lombardi, S.; Catalano, O.; Scuderi, S.; Antonelli, L.A.; Pareschi, G.; Antolini, E.; Arrabito, L.; Bellassai, G.; Bernlöhr, K.; Bigongiari, C.; et al. First detection of the Crab Nebula at TeV energies with a Cherenkov telescope in a dual-mirror Schwarzschild-Couder configuration: The ASTRI-Horn telescope. *A&A* **2020**, *634*, A22. [CrossRef]

13. Scuderi, S.; Giuliani, A.; Pareschi, G.; Tosti, G.; Catalano, O.; Amato, E.; Antonelli, L.A.; Becerra Gonzàles, J.; Bellassai, G.; Bigongiari, C.; et al. The ASTRI Mini-Array of Cherenkov telescopes at the Observatorio del Teide. *J. High Energy Astrophys.* **2022**, *35*, 52–68. [CrossRef]

14. Scuderi, S. The ASTRI Mini-Array: A new pathfinder for Imaging Cherenkov Telescope Arrays. *Universe* **2024**, *submitted*.

15. Vercellone, S.; Bigongiari, C.; Burtovoi, A.; Cardillo, M.; Catalano, O.; Franceschini, A.; Lombardi, S.; Nava, L.; Pintore, F.; Stamerra, A.; et al. ASTRI Mini-Array core science at the Observatorio del Teide. *J. High Energy Astrophys.* **2022**, *35*, 1–42. [CrossRef]

16. Aleksić, J.; Ansoldi, S.; Antonelli, L.A.; Antoranz, P.; Babic, A.; Bangale, P.; Barceló, M.; Barrio, J.A.; Becerra González, J.; Bednarek, W.; et al. The major upgrade of the MAGIC telescopes, Part II: A performance study using observations of the Crab Nebula. *Astropart. Phys.* **2016**, *72*, 76–94. [CrossRef]

17. Holder, J.; Atkins, R.W.; Badran, H.M.; Blaylock, G.; Bradbury, S.M.; Buckley, J.H.; Byrum, K.L.; Carter-Lewis, D.A.; Celik, O.; Chow, Y.C.K.; et al. The first VERITAS telescope. *Astropart. Phys.* **2006**, *25*, 391–401. [CrossRef]

18. De Naurois, M. H.E.S.S.-II—Gamma ray astronomy from 20 GeV to hundreds of TeV's. *Eur. Phys. J. Web Conf.* **2017**, *136*, 03001. [CrossRef]

19. Lombardi, S.; Antonelli, L.A.; Bigongiari, C.; Cardillo, M.; Gallozzi, S.; Green, J.G.; Lucarelli, F.; Saturni, F.G. Performance of the ASTRI Mini-Array at the Observatorio del Teide. In Proceedings of the 37th International Cosmic Ray Conference, Virtual, 12–23 July 2022; p. 884.

20. Zanin, R. (CTAO Observatory, Bologna, Italy) CTAO Project Scientist. Personal Communication, 2021.

21. Abeysekara, A.U.; Alfaro, R.; Alvarez, C.; Álvarez, J.D.; Arceo, R.; Arteaga-Velázquez, J.C.; Avila Rojas, D.; Ayala Solares, H.A.; Barber, A.S.; Bautista-Elivar, N.; et al. The HAWC Real-time Flare Monitor for Rapid Detection of Transient Events. *Astrophys. J.* **2017**, *843*, 116. [CrossRef]

22. Amenomori, M.; Bao, Y.W.; Bi, X.J.; Chen, D.; Chen, T.L.; Chen, W.Y.; Chen, X.; Chen, Y.; Cirennima; Cui, S.W.; et al. First Detection of Photons with Energy beyond 100 TeV from an Astrophysical Source. *Phys. Rev. Lett.* **2019**, *123*, 051101. [CrossRef]

23. di Sciascio, G.; Lhaaso Collaboration. The LHAASO experiment: From Gamma-Ray Astronomy to Cosmic Rays. *Nucl. Part. Phys. Proc.* **2016**, *279-281*, 166–173. [CrossRef]

24. Holler, M.; de Naurois, M.; Zaborov, D.; Balzer, A.; Chalmé-Calvet, R. Photon Reconstruction for H.E.S.S. Using a Semi-Analytical Model. *Int. Cosm. Ray Conf.* **2015**, *34*, 980. [CrossRef]

25. Abeysekara, A.U.; Albert, A.; Alfaro, R.; Alvarez, C.; Álvarez, J.D.; Arceo, R.; Arteaga-Velázquez, J.C.; Ayala Solares, H.A.; Barber, A.S.; Baughman, B.; et al. The 2HWC HAWC Observatory Gamma-Ray Catalog. *Astrophys. J.* **2017**, *843*, 40. [CrossRef]

26. Kawata, K.; Sako, T.K.; Ohnishi, M.; Takita, M.; Nakamura, Y.; Munakata, K. Energy determination of gamma-ray induced air showers observed by an extensive air shower array. *Exp. Astron.* **2017**, *44*, 1–9. [CrossRef]

27. Aharonian, F.; An, Q.; Axikegu; Bai, L.X.; Bai, Y.X.; Bao, Y.W.; Bastieri, D.; Bi, X.J.; Bi, Y.J.; Cai, H.; et al. Observation of the Crab Nebula with LHAASO-KM2A—A performance study. *Chin. Phys. C* **2021**, *45*, 025002. [CrossRef]

28. Cao, Z.; Aharonian, F.A.; An, Q.; Axikegu; Bai, Y.X.; Bao, Y.W.; Bastieri, D.; Bi, X.J.; Bi, Y.J.; Cai, H.; et al. Ultrahigh-energy photons up to 1.4 petaelectronvolts from 12 γ-ray Galactic sources. *Nature* **2021**, *594*, 33–36. [CrossRef]

29. D'Aì, A.; Amato, E.; Burtovoi, A.; Compagnino, A.A.; Fiori, M.; Giuliani, A.; La Palombara, N.; Paizis, A.; Piano, G.; Saturni, F.G.; et al. Galactic observatory science with the ASTRI Mini-Array at the Observatorio del Teide. *J. High Energy Astrophys.* **2022**, *35*, 139–175. [CrossRef]

30. Saturni, F.G.; Arcaro, C.H.E.; Balmaverde, B.; Becerra González, J.; Caccianiga, A.; Capalbi, M.; Lamastra, A.; Lombardi, S.; Lucarelli, F.; Alves Batista, R.; et al. Extragalactic observatory science with the ASTRI mini-array at the Observatorio del Teide. *J. High Energy Astrophys.* **2022**, *35*, 91–111. [CrossRef]

31. Cao, Z.; Aharonian, F.; An, Q.; Axikegu; Bai, Y.X.; Bao, Y.W.; Bastieri, D.; Bi, X.J.; Bi, Y.J.; Cai, J.T.; et al. The First LHAASO Catalog of Gamma-Ray Sources. *arXiv* **2023**, arXiv:2305.17030. [CrossRef].

32. Saturni, F.G.; Lombardi, S.; Antonelli, L.A.; Bigongiari, C.; Fedorova, E.; Giuliani, A.; Lucarelli, F.; Mastropietro, M.; Pareschi, G. Performance of the ASTRI Mini-Array with different levels of the Night Sky Background. In Proceedings of the 38th International Cosmic Ray Conference—PoS(ICRC2023), Nagoya, Japan, 26 July–3 August 2023; Volume 444, p. 717. [CrossRef]

33. Cao, Z.; Aharonian, F.A.; An, Q.; Axikegu; Bai, Y.X.; Bao, Y.W.; Bastieri, D.; Bi, X.J.; Bi, Y.J.; Cai, H.; et al. Peta‚Äielectron volt gamma-ray emission from the Crab Nebula. *Science* **2021**, *373*, 425–430. [CrossRef] [PubMed]

34. Aharonian, F.; An, Q.; Axikegu; Bai, Y.X.; Bao, Y.W.; Bastieri, D.; Bi, X.J.; Bi, Y.J.; Cai, H.; Tian, W.W.; et al. Performance of LHAASO-WCDA and observation of the Crab Nebula as a standard candle. *Chin. Phys. C* **2021**, *45*, 085002. [CrossRef]

35. Punch, M.; Akerlof, C.W.; Cawley, M.F.; Chantell, M.; Fegan, D.J.; Fennell, S.; Gaidos, J.A.; Hagan, J.; Hillas, A.M.; Jiang, Y.; et al. Detection of TeV photons from the active galaxy Markarian 421. *Nature* **1992**, *358*, 477–478. [CrossRef]

36. Ahnen, M.L.; Ansoldi, S.; Antonelli, L.A.; Arcaro, C.; Babić, A.; Banerjee, B.; Bangale, P.; Barres de Almeida, U.; Barrio, J.A.; Becerra González, J.; et al. First multi-wavelength campaign on the gamma-ray-loud active galaxy IC 310. *A&A* **2017**, *603*, A25. [CrossRef]

37. Aleksić, J.; Antonelli, L.A.; Antoranz, P.; Babic, A.; Barres de Almeida, U.; Barrio, J.A.; Becerra González, J.; Bednarek, W.; Berger, K.; Bernardini, E.; et al. Rapid and multiband variability of the TeV bright active nucleus of the galaxy IC 310. *A&A* **2014**, *563*, A91. [CrossRef]

38. MAGIC Collaboration; Acciari, V.A.; Ansoldi, S.; Antonelli, L.A.; Arbet Engels, A.; Arcaro, C.; Baack, D.; Babić, A.; Banerjee, B.; Bangale, P.; et al. Monitoring of the radio galaxy M 87 during a low-emission state from 2012 to 2015 with MAGIC. *MNRAS* **2020**, *492*, 5354–5365. [CrossRef]

39. Aharonian, F.; Akhperjanian, A.G.; Bazer-Bachi, A.R.; Beilicke, M.; Benbow, W.; Berge, D.; Bernlöhr, K.; Boisson, C.; Bolz, O.; Borrel, V.; et al. Fast Variability of Tera-Electron Volt γ Rays from the Radio Galaxy M87. *Science* **2006**, *314*, 1424–1427. [CrossRef] [PubMed]

40. Aliu, E.; Arlen, T.; Aune, T.; Beilicke, M.; Benbow, W.; Bouvier, A.; Bradbury, S.M.; Buckley, J.H.; Bugaev, V.; Byrum, K.; et al. VERITAS Observations of Day-scale Flaring of M 87 in 2010 April. *Astrophys. J.* **2012**, *746*, 141. [CrossRef]

41. Biteau, J.; Prandini, E.; Costamante, L.; Lemoine, M.; Padovani, P.; Pueschel, E.; Resconi, E.; Tavecchio, F.; Taylor, A.; Zech, A. Progress in unveiling extreme particle acceleration in persistent astrophysical jets. *Nat. Astron.* **2020**, *4*, 124–131. [CrossRef]

42. Galanti, G.; Roncadelli, M. Behavior of axionlike particles in smoothed out domainlike magnetic fields. *Phys. Rev. D* **2018**, *98*, 043018. [CrossRef]

43. Alves Batista, R.; Saveliev, A. The Gamma-Ray Window to Intergalactic Magnetism. *Universe* **2021**, *7*, 223. [CrossRef]

44. Tavecchio, F.; Romano, P.; Landoni, M.; Vercellone, S. Putting the hadron beam scenario for extreme blazars to the test with the Cherenkov Telescope Array. *MNRAS* **2019**, *483*, 1802–1807. [CrossRef]

45. Acciari, V.A.; Ansoldi, S.; Antonelli, L.A.; Arbet Engels, A.; Asano, K.; Baack, D.; Babić, A.; Baquero, A.; Barres de Almeida, U.; Barrio, J.A.; et al. MAGIC Observations of the Nearby Short Gamma-Ray Burst GRB 160821B. *Astrophys. J.* **2021**, *908*, 90. [CrossRef]

46. Abdalla, H.; Adam, R.; Aharonian, F.; Ait Benkhali, F.; Angüner, E.O.; Arakawa, M.; Arcaro, C.; Armand, C.; Ashkar, H.; Backes, M.; et al. A very-high-energy component deep in the γ-ray burst afterglow. *Nature* **2019**, *575*, 464–467. [CrossRef]

47. MAGIC Collaboration; Acciari, V.A.; Ansoldi, S.; Antonelli, L.A.; Arbet Engels, A.; Baack, D.; Babić, A.; Banerjee, B.; Barres de Almeida, U.; Barrio, J.A.; et al. Teraelectronvolt emission from the γ-ray burst GRB 190114C. *Nature* **2019**, *575*, 455–458. [CrossRef]

48. H. E. S. S. Collaboration; Abdalla, H.; Aharonian, F.; Ait Benkhali, F.; Angüner, E.O.; Arcaro, C.; Armand, C.; Armstrong, T.; Ashkar, H.; Backes, M.; et al. Revealing X-ray and gamma ray temporal and spectral similarities in the GRB 190829A afterglow. *Science* **2021**, *372*, 1081–1085. [CrossRef]

49. Suda, Y.; Artero, M.; Asano, K.; Berti, A.; Nava, L.; Noda, K.; Terauchi, K.; Acciari, V.A.; Ansoldi, S.; Antonelli, L.A.; et al. Observation of a relatively low luminosity long duration GRB 201015A by the MAGIC telescopes. In Proceedings of the 37th International Cosmic Ray Conference, Virtual, 12–23 July 2022; p. 797. [CrossRef]

50. Fukami, S.; Berti, A.; Loporchio, S.; Suda, Y.; Nava, L.; Noda, K.; Bošnjak, Ž.; Asano, K.; Longo, F.; The MAGIC Collaboration; et al. Very-high-energy gamma-ray emission from GRB 201216C detected by MAGIC. In Proceedings of the 37th International Cosmic Ray Conference, Virtual, 12–23 July 2022; p. 788. [CrossRef]

51. Huang, Y.; Hu, S.; Chen, S.; Zha, M.; Liu, C.; Yao, Z.; Cao, Z.; Experiment, T.L. LHAASO observed GRB 221009A with more than 5000 VHE photons up to around 18 TeV. *GRB Coord. Netw.* **2022**, *32677*, 1.

52. Burns, E.; Svinkin, D.; Fenimore, E.; Kann, D.A.; Agüí Fernández, J.F.; Frederiks, D.; Hamburg, R.; Lesage, S.; Temiraev, Y.; Tsvetkova, A.; et al. GRB 221009A: The Boat. *Astrophys. J. Lett.* **2023**, *946*, L31. [CrossRef]

53. LHAASO Collaboration; Cao, Z.; Aharonian, F.; An, Q.; Axikegu; Bai, L.X.; Bai, Y.X.; Bao, Y.W.; Bastieri, D.; Bi, X.J.; et al. A tera-electron volt afterglow from a narrow jet in an extremely bright gamma-ray burst. *Science* **2023**, *380*, 1390–1396. [CrossRef] [PubMed]

54. Cao, Z.; Aharonian, F.; An, Q.; Axikegu; Bai, Y.X.; Bao, Y.W.; Bastieri, D.; Bi, X.J.; Bi, Y.J.; Cai, J.T.; et al. Very high-energy gamma-ray emission beyond 10 TeV from GRB 221009A. *Sci. Adv.* **2023**, *9*, eadj2778. [CrossRef]
55. Galanti, G.; Roncadelli, M.; Tavecchio, F. Assessment of ALP scenarios for GRB 221009A. *arXiv* **2022**, arXiv:2211.06935. [CrossRef].
56. Galanti, G.; Nava, L.; Roncadelli, M.; Tavecchio, F.; Bonnoli, G. Observability of the Very-High-Energy Emission from GRB 221009A. *Phys. Rev. Lett.* **2023**, *131*, 251001. [CrossRef]
57. IceCube Collaboration; Abbasi, R.; Ackermann, M.; Adams, J.; Aguilar, J.A.; Ahlers, M.; Ahrens, M.; Alameddine, J.M.; Alispach, C.; Alves, A.A., Jr.; et al. Evidence for neutrino emission from the nearby active galaxy NGC 1068. *Science* **2022**, *378*, 538–543. [CrossRef]
58. Lamastra, A.; Fiore, F.; Guetta, D.; Antonelli, L.A.; Colafrancesco, S.; Menci, N.; Puccetti, S.; Stamerra, A.; Zappacosta, L. Galactic outflow driven by the active nucleus and the origin of the gamma-ray emission in NGC 1068. *A&A* **2016**, *596*, A68. [CrossRef]
59. Acciari, V.A.; Ansoldi, S.; Antonelli, L.A.; Arbet Engels, A.; Baack, D.; Babić, A.; Banerjee, B.; Barres de Almeida, U.; Barrio, J.A.; Becerra González, J.; et al. Constraints on Gamma-Ray and Neutrino Emission from NGC 1068 with the MAGIC Telescopes. *Astrophys. J.* **2019**, *883*, 135. [CrossRef]
60. Zampieri, L.; Bonanno, G.; Bruno, P.; Gargano, C.; Lessio, L.; Naletto, G.; Paoletti, L.; Rodeghiero, G.; Romeo, G.; Bulgarelli, A.; et al. A stellar intensity interferometry instrument for the ASTRI Mini-Array telescopes. In *Optical and Infrared Interferometry and Imaging VIII*; Mérand, A., Sallum, S., Sanchez-Bermudez, J., Eds.; Society of Photo-Optical Instrumentation Engineers (SPIE) Conference Series; SPIE: Bellingham, WA, USA, 2022; Volume 12183, p. 121830F. [CrossRef]
61. Egron, E.; Pellizzoni, A.; Iacolina, M.N.; Loru, S.; Marongiu, M.; Righini, S.; Cardillo, M.; Giuliani, A.; Mulas, S.; Murtas, G.; et al. Imaging of SNR IC443 and W44 with the Sardinia Radio Telescope at 1.5 and 7 GHz. *MNRAS* **2017**, *470*, 1329–1341. [CrossRef]
62. Loru, S.; Pellizzoni, A.; Egron, E.; Righini, S.; Iacolina, M.N.; Mulas, S.; Cardillo, M.; Marongiu, M.; Ricci, R.; Bachetti, M.; et al. Investigating the high-frequency spectral features of SNRs Tycho, W44, and IC443 with the Sardinia Radio Telescope. *MNRAS* **2019**, *482*, 3857–3867. [CrossRef]
63. Bortoletto, F.; Bonoli, C.; D'Alessandro, M.; Ragazzoni, R.; Conconi, P.; Mancini, D.; Pucillo, M. Commissioning of the Italian National Telescope Galileo. In *Advanced Technology Optical/IR Telescopes VI*; Stepp, L.M., Ed.; Society of Photo-Optical Instrumentation Engineers (SPIE) Conference Series; SPIE: Bellingham, WA, USA, 1998; Volume 3352, pp. 91–101. [CrossRef]
64. Villata, M.; Raiteri, C.M.; Larionov, V.M.; Kurtanidze, O.M.; Nilsson, K.; Aller, M.F.; Tornikoski, M.; Volvach, A.; Aller, H.D.; Arkharov, A.A.; et al. Multifrequency monitoring of the blazar 0716+714 during the GASP-WEBT-AGILE campaign of 2007. *A&A* **2008**, *481*, L79–L82. [CrossRef]
65. Predehl, P.; Andritschke, R.; Arefiev, V.; Babyshkin, V.; Batanov, O.; Becker, W.; Böhringer, H.; Bogomolov, A.; Boller, T.; Borm, K.; et al. The eROSITA X-ray telescope on SRG. *A&A* **2021**, *647*, A1. [CrossRef]
66. Weisskopf, M.C.; Ramsey, B.; O'Dell, S.; Tennant, A.; Elsner, R.; Soffitta, P.; Bellazzini, R.; Costa, E.; Kolodziejczak, J.; Kaspi, V.; et al. The Imaging X-ray Polarimetry Explorer (IXPE). In *Space Telescopes and Instrumentation 2016: Ultraviolet to Gamma Ray*; den Herder, J.W.A., Takahashi, T., Bautz, M., Eds.; SPIE: Bellingham, WA, USA, 2016; Society of Photo-Optical Instrumentation Engineers (SPIE) Conference Series; Volume 9905, p. 990517. [CrossRef]
67. Albert, A.; Alfaro, R.; Alvarez, C.; Camacho, J.R.A.; Arteaga-Velázquez, J.C.; Arunbabu, K.P.; Avila Rojas, D.; Ayala Solares, H.A.; Baghmanyan, V.; Belmont-Moreno, E.; et al. 3HWC: The Third HAWC Catalog of Very-high-energy Gamma-Ray Sources. *Astrophys. J.* **2020**, *905*, 76. [CrossRef]
68. LHAASO Collaboration. An ultrahigh-energy γ-ray bubble powered by a super PeVatron. *Sci. Bull.* **2024**, *69*, 449–457. [CrossRef] [PubMed]
69. Chernyakova, M.; Malyshev, D.; Paizis, A.; La Palombara, N.; Balbo, M.; Walter, R.; Hnatyk, B.; van Soelen, B.; Romano, P.; Munar-Adrover, P.; et al. Overview of non-transient γ-ray binaries and prospects for the Cherenkov Telescope Array. *A&A* **2019**, *631*, A177. [CrossRef]
70. Pintore, F.; Giuliani, A.; Belfiore, A.; Paizis, A.; Mereghetti, S.; La Palombara, N.; Crestan, S.; Sidoli, L.; Lombardi, S.; D'Aì, A.; et al. Scientific prospects for a mini-array of ASTRI telescopes: A γ-ray TeV data challenge. *J. High Energy Astrophys.* **2020**, *26*, 83–94. [CrossRef]
71. Aharonian, F.; Akhperjanian, A.G.; Bazer-Bachi, A.R.; Beilicke, M.; Benbow, W.; Berge, D.; Bernlöhr, K.; Boisson, C.; Bolz, O.; Borrel, V.; et al. 3.9 day orbital modulation in the TeV γ-ray flux and spectrum from the X-ray binary LS 5039. *A&A* **2006**, *460*, 743–749. [CrossRef]
72. Quinn, J.; Akerlof, C.W.; Biller, S.; Buckley, J.; Carter-Lewis, D.A.; Cawley, M.F.; Catanese, M.; Connaughton, V.; Fegan, D.J.; Finley, J.P.; et al. Detection of Gamma Rays with E > 300 GeV from Markarian 501. *Astrophys. J.* **1996**, *456*, L83. [CrossRef]
73. MAGIC Collaboration; Acciari, V.A.; Ansoldi, S.; Antonelli, L.A.; Babić, A.; Banerjee, B.; Barres de Almeida, U.; Barrio, J.A.; Becerra González, J.; Bednarek, W.; et al. Study of the variable broadband emission of Markarian 501 during the most extreme Swift X-ray activity. *A&A* **2020**, *637*, A86. [CrossRef]
74. Lamastra, A.; Tavecchio, F.; Romano, P.; Landoni, M.; Vercellone, S. Unveiling the origin of the gamma-ray emission in NGC 1068 with the Cherenkov Telescope Array. *Astropart. Phys.* **2019**, *112*, 16–23. [CrossRef]
75. ASTRI Project, ASTRI Mini-Array Instrument Response Functions (Prod2, v1.0). 2022. Available online: https://zenodo.org/records/6827882 (accessed on 21 January 2024). [CrossRef]

76. Knödlseder, J.; Mayer, M.; Deil, C.; Cayrou, J.B.; Owen, E.; Kelley-Hoskins, N.; Lu, C.C.; Buehler, R.; Forest, F.; Louge, T.; et al. GammaLib and ctools. A software framework for the analysis of astronomical gamma-ray data. *A&A* **2016**, *593*, A1. [CrossRef]
77. Donath, A.; Terrier, R.; Remy, Q.; Sinha, A.; Nigro, C.; Pintore, F.; Khélifi, B.; Olivera-Nieto, L.; Ruiz, J.E.; Brügge, K.; et al. Gammapy: A Python package for gamma-ray astronomy. *A&A* **2023**, *678*, A157. [CrossRef]